



21st European Conference on Fracture, ECF21, 20-24 June 2016, Catania, Italy

## Fatigue of NiTi shape memory wires

Sebastián M. Jaureguizar<sup>a</sup>, Mirco D. Chapetti<sup>b\*</sup> and Alejandro A. Yawny<sup>a</sup>

<sup>a</sup>*División Física de Metales, Centro Atómico Bariloche, CNEA-CONICET, Av. Bustillo 9500, S.C. Bariloche (8400), Argentina*

<sup>b</sup>*INTEMA (CONICET-Universidad Nacional de Mar del Plata, FI), J.B. Justo 4302, Mar del Plata (7600), Argentina*

---

### Abstract

In the present work, an innovative methodology for characterizing structural fatigue of NiTi superelastic wires is proposed. It consists in, firstly, performing low speed nearly isothermal pseudoelastic cycles in a limited region of the wire specimen. This results in the stabilization of the pseudoelastic behavior accompanied by a decrease in the stresses for forward and reverse transformations which allows obtaining an equivalent to a geometric dog-bone shaped specimen due to the reduced transformation stresses in the pre-cycled region. In a second stage, by limiting the transformation active zone to the pre-cycled region, the deformation speed can be increased to practical values avoiding any transformation activity outside that region. In that way, grip induced failures resulting in artificially shorter fatigue lives might be completely avoided thus allowing an accurate characterization of the true structural fatigue. Additionally, strain controlled experiments on wires in fully austenite and fully martensite states have been performed. Resulting fatigue lives in these cases were at least two orders of magnitude higher compared with the pseudoelastic fatigue indicating the decisive role played by the stress induced transformation in determining fatigue life. The influence of testing temperature and deformation rate on fatigue life has also been evaluated

© 2016, PROSTR (Procedia Structural Integrity) Hosting by Elsevier Ltd. All rights reserved.  
Peer-review under responsibility of the Scientific Committee of PCF 2016.

*Keywords:* shape memory NiTi wires; pull-pull fatigue test; pseudoelasticity.

---

### 1. Introduction

Superelasticity is the capacity by which some shape memory alloys (SMA) are able to be strained up to nearly 8-10% in a reversible manner. A hysteretic behavior associated with the stress-strain response is observed with the reverse transformation occurring at a lower stress level than the forward transformation [Miyazaki et al (1981-a)].

---

\* Corresponding author. Tel.: +54-223-4816600; fax: +54-223-4810046.  
E-mail address: [mchapetti@fi.mdp.edu.ar](mailto:mchapetti@fi.mdp.edu.ar)

Fatigue is an important issue in applications based on the pseudoelastic behavior where the stress induced transformation is induced repeatedly. This is also the case with NiTi shape memory alloys on which most of the practical applications are based, and particularly in superelastic NiTi wires which are used in a wide variety of devices ranging from medical tooling to damping systems.

There is a lack in the literature of information concerning the appropriate characterization of the intrinsic structural fatigue life of SMA elements under pseudoelastic nearly isothermal cycling conditions. This information could then be used in design procedures for more complex working conditions using appropriate modification factors, paralleling classical fatigue treatment. In effect, most of the data available in the literature correspond to the particular conditions associated with specific applications and the corresponding results cannot be easily extended to other particular cases. For example, due to its importance in medical tooling applications, rotary bending fatigue experiments performed at high cycling frequencies have been considered by many authors [Miyazaki et al. (1999), Sawaguchi et al. [2003], Rahim et al. (2013), Pelton et al. (2013)]. Under these circumstances, complex stress states and temperature effects associated with the exothermic–endothermic character of the involved phase transformations are introduced.

Therefore, there is a need of generating experimental information from simple tests performed under well-defined conditions. In the present work, an alternative method for accurate evaluation of the intrinsic fatigue properties of NiTi wires under pseudoelastic cycling conditions is developed. The testing procedure here proposed eliminates the need of using typical dog-bone shaped specimens in order to avoid the grip - specimen singularities where the fatigue damage can be localized. Obtaining dog-bone shaped specimens in thin wires could be, on the one hand, relatively unpractical. On the other hand, the surface and subsurface characteristics resulting from a particular wire fabrication route that are determinant in the resulting fatigue life are eliminated as a consequence of the machining procedure. This is undesirable if the intrinsic fatigue resistance wants to be characterized.

The proposed test methodology was applied to characterize the structural fatigue life of a commercial ultrafine grained NiTi wire [Yawny et al. (2005)]. In addition, and for comparison purposes, strain controlled experiments were performed in wires in fully austenite and fully martensite states. Resulting fatigue lives in these cases were at least two orders of magnitude higher compared with the pseudoelastic fatigue. This indicates the decisive role played by the stress induced transformation in determining fatigue life. The influence of testing temperature and deformation rate on fatigue life has been also evaluated.

## 2. Material and Fatigue Testing

A 0.5 mm in diameter commercial (SAES Getters) Ni rich NiTi (50.9 at.% Ni) superelastic wire was used in the present study. It possess an ultrafine grained microstructure (grain size 40-50 nm) as a result of a straight annealing procedure performed after a cold work area reduction of nearly 45% by wire drawing. Surface condition was black oxide. The austenite phase was stable at ambient temperature and the  $A_f$  temperature was  $-15\text{ }^\circ\text{C}$  for the fully annealed condition according to manufacturer's specification and around room temperature for the straight annealed condition as determined by standard four leads electric resistivity measurement.

Fatigue cycling was performed using servohydraulic testing machines MTS 810 and INSTRON 8800 equipped with respective environmental chambers. Tests were conducted under crosshead displacement control at crosshead speed of 0.1 or 1.0 mm/min. The gripping device used in the fatigue experiments is illustrated in Fig. 1. It corresponds to the snubbing type of device recommended in ASTM E8 [ASTM E8 (2013)] for testing thin wires and was selected here because it provides a more gentle gripping action in comparison with classical wedge type gripping devices. This is an important factor contributing to eradicate early failures induced by grip-specimen interaction. The diameter of both gripping pulleys was 50 mm which results in an initial strain of 0.5 %, well below the 1 % strain value characteristic of the stress induced transformation in NiTi [Iadicola and Shaw (2007)]. Pseudoelastic tests were performed at constant controlled temperatures of  $T = 25\text{ }^\circ\text{C}$ ,  $37\text{ }^\circ\text{C}$  and  $50\text{ }^\circ\text{C}$ .

In addition, for comparison purposes strain controlled experiments on wires in fully austenite and fully martensite states have been performed at constant controlled temperature of  $T = 37\text{ }^\circ\text{C}$ .

Wire specimens with a total length of 140 mm were used for fatigue testing. The free length between grips was  $L_0 = 60\text{ mm}$ . An equivalent strain rate can be estimated by dividing the above mentioned imposed crosshead

displacement rates by  $L_0$  giving values of  $1.67 \cdot 10^{-3} \text{ min}^{-1}$  ( $2.77 \cdot 10^{-5} \text{ s}^{-1}$ ) and  $1.67 \cdot 10^{-2} \text{ min}^{-1}$  ( $2.77 \cdot 10^{-4} \text{ s}^{-1}$ ), respectively. An average applied strain  $\epsilon_{CH}$  was calculated by dividing the crosshead displacement by  $L_0$ .

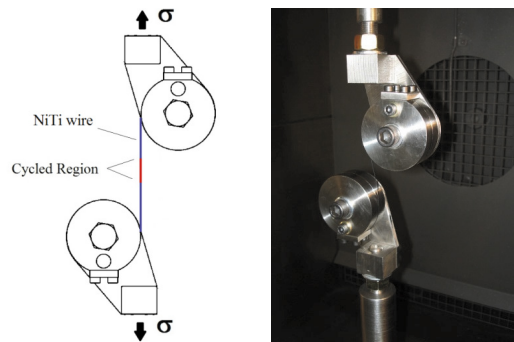


Fig. 1. Snubbing type of gripping device used for fatigue testing.

### 3. “Virtual Dog-Bone” specimen for pseudoelastic fatigue

In order to ensure that the pure fatigue damage be localized in a free zone of the wire far from the influence of the grips, a geometric dog-bone shaped specimen is used in fatigue testing of standard structural materials. In most of the cases, the shape is obtained by machining or grinding. In the case of small diameters wires or when the surface of the components is part of the configuration to be analyzed, this procedure is neither possible nor recommendable.

In the superelastic NiTi wire material, an equivalent to a geometric dog-bone specimen can be generated. It will be referred to as “virtual dog-bone” specimen (VDB) in what follows. In order to get such a specimen, advantage is taken of the localized nature of the stress induced transformation in the used NiTi wires which proceeds by the movement of a finite number of transformation fronts [Olbricht et al. (2008)]. Fig. 2 illustrates schematically the pseudoelastic behavior of a NiTi wire [Olbricht et al. (2008), Yawny et al. (2008)] and the basis of the proposal. The black line corresponds to the first imposed cycle while the red one is obtained after a certain number of cycles (100 in the present case). The overstress observed in cycle 1 and cycle 100 represented in Fig. 3 corresponds to the nucleation of a new transforming domain [Soul et al. (2013), Iadicola and Shaw (2007)]. The decrease in the critical stress associated with the loading plateau is especially noticeable within the first 100 pseudoelastic cycles. This type of evolution of the properties associated with the repeated stress induced transformation belongs to what is known as functional fatigue, in opposition to structural fatigue conducting to fracture failure [Eggeler et al. (2004)]. The effects of functional fatigue can be concentrated in a certain zone of the material because, as mentioned before, the stress induced transformation proceeds by the movement of a finite number of transformation. Therefore, the proposal is to perform 100 pseudoelastic cycles in a certain region of the material. After this first cycling stage is completed, the sample is completely unloaded and then reloaded. In that way, it is ensured that the new stress induced martensitic transformation will nucleate and proceed only in the pre-cycled zone, if the maximum strain is controlled. This is possible because the reduction in the critical stress is higher than the overstress necessary to nucleate a new transforming domain [Soul et al. (2013), Iadicola and Shaw (2007)].

Fig. 2 also shows schematically the method proposed to create a VDB specimen. Blue and green lines in Fig. 2 represent the expected behavior of the stresses when loading and unloading the sample with total transformation for cycle number 1 and 100, respectively. At first, the specimen is tensile stressed and then partially retransformed up to point 4 ( $\epsilon_{\min}$ ). The unloading generates first an elastic decrease in stress and then the plateau of reverse transformation takes place until the strain  $\epsilon_{\min}$  is reached (point 4 in Fig. 2). The first cycle is then finished ( $N = 1$ ). Once the first cycle is finished at point 4, cycling is continued by imposing a constant strain range  $\Delta\epsilon_c$  given by  $\epsilon_{\min}$  and  $\epsilon_{\max}$ , at the same crosshead speed. Due to functional fatigue, the applied stress range will decrease with the number of cycles until the cycle represented by the red line ( $N = 100$ ) in Fig. 2 is reached. For the cycle number 100, the minimum and maximum stress levels will be given by points 5 and 6 respectively. It is important to mention here

that critical stresses obtained after 100 cycles of partial transformation are the same as those obtained after cycling through the complete transformation [Miyazaki et al. (1981), Yawny et al. (2005)].

After the 100 cycles are completed, the VDB specimen is created and the pseudoelastic fatigue test for the intrinsic fatigue analysis can be then started.

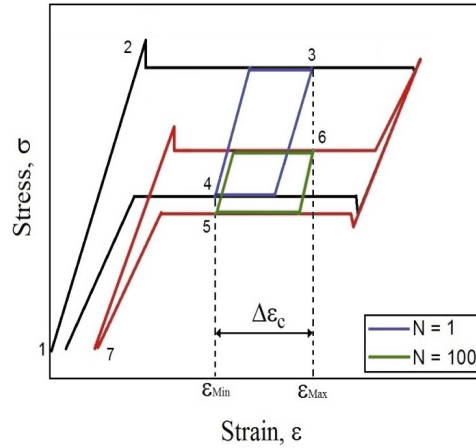


Fig. 2. Scheme of pseudoelastic behavior of the NiTi wire and the proposed experimental procedure for the VDB specimen generation.

Fig. 3 illustrates the procedure in a real specimen. For the generation of the VDB specimen, tests were conducted at a crosshead displacement rate of 0.1 mm/min and the measured strains and stresses for one of the tests and for the first and the final cycles are shown in Fig. 3(a). The cycle referred to cycle “0” represents a reference complete cycle with a maximum strain of 5.66 %. Then, the sample was unloaded to strain value of 4.06 %. The strain amplitude related to these values corresponds to approximately an active length of the wire of 10 mm (effective test length,  $L_{eff}$ ). Once reaching a deformation of 4.06 % cycling was started. After completing cycle number 101, the specimen was unloaded as shown in Fig. 3(a). Once the VDB specimen is obtained, and before starting the fatigue test, cycle 102 is performed at 0.1 mm/min in order to verify that the transformation starts in the desired zone. After that, the fatigue test is started, applying a crosshead displacement rate of 1 mm/min (equivalent strain rate  $2.77 \cdot 10^{-4} \text{ s}^{-1}$ ). Fig. 3(b) shows the stress-strain values for cycles number 102, 122, 2000 and 11750 (the last before fracture). A quasistatic complete pseudoelastic cycle corresponding to a wire without functional fatigue (black dashed line) is superimposed as a reference.

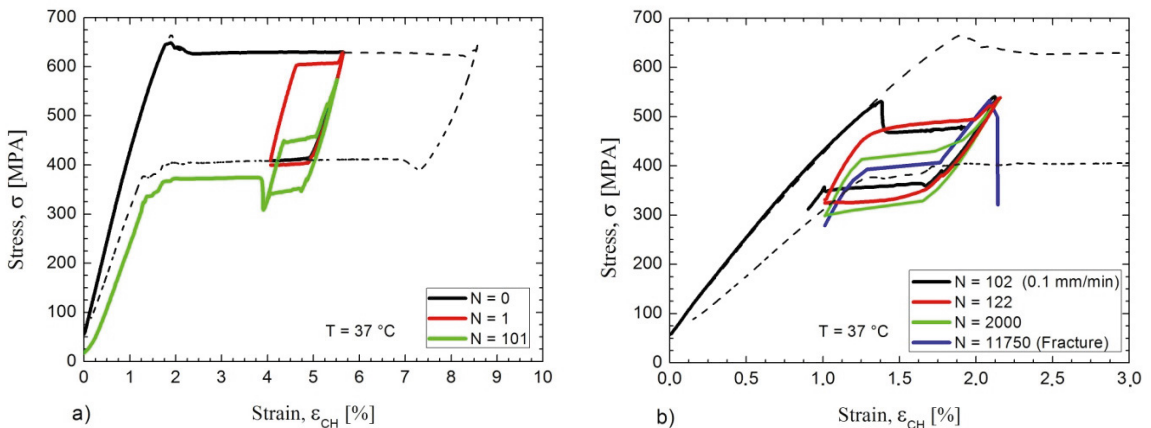


Fig. 3. Pseudoelastic cycling: (a) Creating the VDB Specimen. (b) Fatigue test.

#### 4. Results and discussion

In all pseudoelastic tests fracture took place in free length between grips in the cycled region, which shows that the proposed methodology locates the damage in the zone of interest, away from the area of grips. This validates the results obtained in terms of intrinsic resistance. Table 1 summarizes the experimental conditions and the fatigue lives  $N_f$  obtained. As it can be observed, fatigue lives differed below 61% in all cases and temperatures.

In Table 2, the cycling parameters and the resulting fatigue lives corresponding to the fatigue experiments performed in austenite and martensite, i.e., without pseudoelastic transformation are summarized.

Table 1. Pseudoelastic cycling parameters and resulting fatigue lives

Temperature [°C]	$\Delta\varepsilon$ [%]	$\sigma_{\max}$ [MPa]	$\sigma_a$ [MPa]	Number of cycles to fracture, $N_f$
25	1.16	518	199	13,597
	1.16	513	190	7,235
	2.29	513	180	10,685
	3.51	480	181	8,902
37	1.16	542	126	11,750
	1.15	568	135	6,418
	2.32	553	149	6,805
	2.29	561	155	7,442
	4.64	551	156	8,600
50	3.74	562	165	8,940
	1.14	712	110	10,600
	2.28	661	152	5,178
	3.35	733	139	9,176

Table 2. Cycling test parameters and resulting fatigue lives for tests without transformation.

Material States	Specimen	$\varepsilon_{\text{mean}}$ (%)	$\varepsilon_a$ (%)	$\sigma_{\max}$ (MPa)	$\sigma_a$ (MPa)	Number of cycles to fracture, $N_f$
Austenite	A	1.80	0.10	587	89	> 10,000,000
	B	1.37	0.11	595	82	> 7,000,000
	C	1.46	0.09	581	74	> 10,000,000
Martensite	D	7.87	0.24	598	85	895,015
	E	8.15	0.19	596	83	932,956
	F	8.12	0.26	590	83	566,954

The applied strain amplitude was defined such that the applied stress amplitude ( $\sigma_{\max} - \sigma_{\min}$ ) remained within the transformation and retransformation plateaus corresponding to an ambient temperature of 37 °C. This can be observed in Fig. 4, where representative cycles for both conditions, i.e., austenite and martensite stress-induced phases, have been included. Fig 4 also shows a complete pseudoelastic cycle at a displacement rate of 0.1 mm/min at the same temperature (37°C) as a reference. In all cases, the mean strain was configured in the first loading cycle, and no significant hysteresis was observed. Finally, Fig. 4 shows an example of a cycle of a test performed at 37 °C using a VDB specimen.

Specimens cycled in austenite phase experienced a fatigue life above the  $7 \times 10^6$  cycles before fracture (run-out). Furthermore, in those samples in martensite phase where fracture occurred, the process began in areas in close contact with grips; then, it is not possible to assure that the resulting fatigue lives obtained are intrinsic and exclusively associated to fatigue damage. In those cases, longer intrinsic fatigue lives are expected.

Fig. 5 shows the applied strain ranges vs. the number of cycles for pseudoelastic tests performed at 25 °C, 37 °C and 50 °C, temperatures. As a reference, the average strain-life curve for various high-strength Ti alloys is also included [Meggiolaro (2004)]. The values that correspond to the cycling without transformation (austenite or martensite phase), with fatigue lives two or three orders of magnitude higher, appear in Fig. 5 as run-outs.

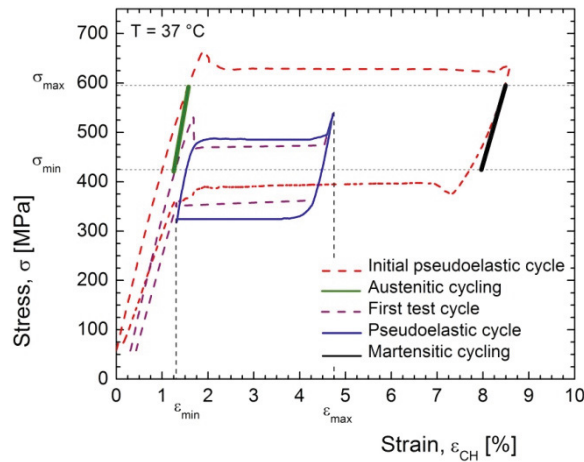


Fig. 4. All test types performed.

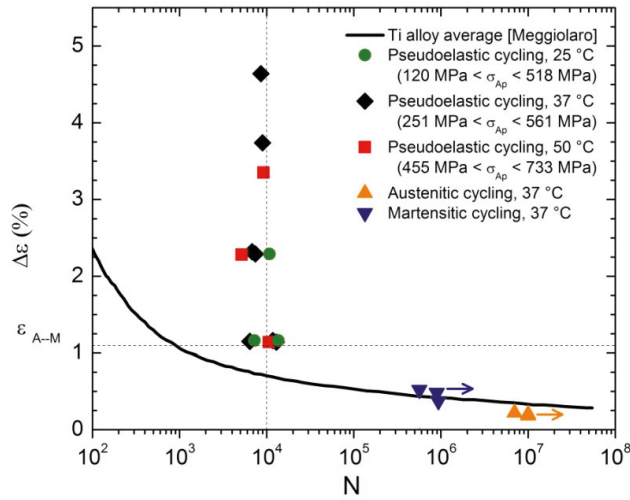


Fig. 5. All test results.

From the analysis of results it can be assumed that above the initial strain of the martensitic transformation, fatigue life does not depend on the applied strain range, nor on the mean strain; but basically on the number of cyclic transformations experienced by the wire. Resulting fatigue lives are clearly around the 10,000 cycles for the analyzed NiTi wire, independently of the applied strain range. Results clearly contradict several bibliographical reports, which postulate a relation between fatigue life (number of cycles to fracture of the wire or component) and the applied strain range and use Coffin-Manson type models [Melton and Mercier (1979), Lagoudas et al. (2009), Kollerov et al. (2013)]. Present results, together with the proposed testing methodology that allows the analysis of the intrinsic fatigue resistance of the wire, will lead to thorough analysis of the damage mechanism and the variables that control it.

Another important finding is the independence of fatigue life on the test temperature, which defines the applied stress range and the load ratio (see Table 2 and Fig. 5). This shows that the number of transformation cycles is the decisive factor determining fatigue life and indicates that a great amount of cumulative damage is introduced in the wire every time the transformation front sweeps a particular zone.

It is also important to analyze the effect of strain rate in the study of fatigue life. Some authors have studied the effect of rotational speed in roto-bending tests [Eggeler et al. (2004), Sawaguchi et al. (2003), Wagner et al. (2004)]. Sawaguchi et al. show that the fatigue life (number of cycles to fracture) decreases with the increase of rotational speed, and that above 400 rpm the effect vanishes. Wagner et al. proposes, as answer to this effect, that the increase of the wire temperature is a function of the rotational speed. Eggeler et al. relates thermal effects and the relation of transformation stresses with temperature (Clausius-Clapeyron), concluding that by increasing strain rate, the applied stress can be significantly increased as well. These bibliographical results sustain the proposal of the test methodology presented in the present work. All results reported in the bibliography, and in particular those obtained from fatigue tests performed with the roto-bending method and its variations, are carried out at high speed, without considering thermal effects [Miyazaki et al. (1999), Kim (2002), Sawaguchi et al. (2003), Wagner et al. (2004), Kollerov et al. (2013), Pelton et al. (2013), Rahim et al. (2013)].

Results in Fig. 5 were obtained at a strain rate of 0.0167 1/min which can be assumed corresponds to a quasi-static isothermal test. Fig. 6 shows all results included in Fig. 5 as well as those reported by Sawaguchi et al. and Wagner et al. It is important to note that roto-bending tests apply alternative cycles with a zero load ratio; i.e., a tensile transformation cycle and a compressive transformation cycle are applied in each cycle; thus two transformation cycles should be considered for every loading cycle. This is of great importance if the number of transformation cycles becomes a determinant variable when calculating the amount of fatigue damage in NiTi wires. For this reason, two transformations per cycle are considered in these cases in order to compare results. It is also important to analyze that the strain rate of each roto-bending test varies with the applied strain amplitude. For comparison purposes, a mean strain rate was obtained for every applied rotation speed. Values oscillate between 1.4 1/min and 26.4 1/min (see Fig. 6).

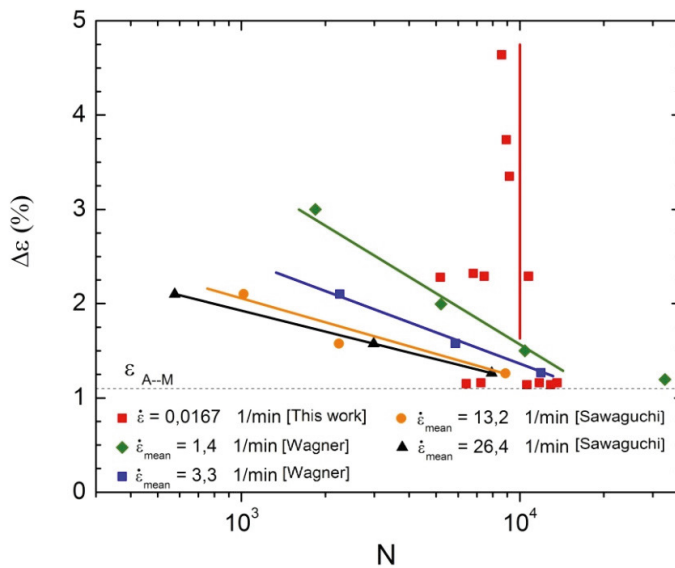


Fig. 6. Effects of strain rate in fatigue life.

Fig. 6 shows that by decreasing strain rate and by cycling above the initial strain of the martensite transformation ( $\epsilon_{A-M}$ ), the dependence of fatigue life on the applied strain range decreases. These results show the importance of studying the intrinsic resistance of the NiTi wire by means of quasi-static tests and using a homogeneous strain rate along the effective test volume. This would also allow a further study on the microstructural variables involved in the resistance to fatigue, as for instance the influence of type and size of existing inclusions in the microstructure. Therefore, if strain rate has certain influence on the damage mechanism and the resulting fatigue life, the comparison of results from flexo-rotating tests turns invalid when analyzing the intrinsic resistance of the material as a function of the applied strain range.

## 5. Conclusions

A new test method for characterizing uniaxial pull-pull intrinsic pseudoelastic fatigue life of commercial NiTi wires is proposed. It is based in obtaining a “virtual dog-bone” shaped specimen by performing first 100 low speed displacement controlled pseudoelastic cycles in a reduced portion of the specimen. The proposed test method was applied to analyze commercial superelastic NiTi wire ultrafine grained with a diameter of 0.5 mm. Pseudoelastic cycling tests were carried out at different ambient temperatures and several strain amplitudes in order to study their effect on fatigue life.

Fatigue life was shown not to depend on the applied strain range or on the mean strain. Resulting fatigue lives for the wire under study are clearly near the 10,000 cycles, independently of the applied strain range. Even if cycle tests at very low strain rate take a long time, they would allow obtaining a highly important resistance value of reference for the study of the intrinsic damage mechanism of the material associated to pseudoelastic cycling. Future analysis of fatigue of NiTi wires should not ignore this issue.

## Acknowledgements

Authors wish to express their gratitude to the funding provided by CONICET, ANPCyT, and SeCTyP UNCuyo.

## References

- ASTM E8, Standard Test Methods for Tension Testing of Metallic Materials, ASTM International, 2013.
- Eggeler, G., Hornbogen, E., Yawny, A., Heckmann, A., Wagner, M., 2004. Structural and functional fatigue of NiTi shape memory alloys. *Mater.Sci. Eng. A* 378, 24–33.
- Iadicola, M. A., Shaw, J. A., 2007. An experimental method to measure initiation events during unstable stress-induced martensitic transformation in a shape memory alloy wire. *Smart Mater. Struct.* 16, S155–S169.
- Kim, Y., 2012. Fatigue Properties of the Ti-Ni Base Shape Memory Alloy Wire., *Mater. Trans.* 43, 1703–1706.
- Kollerov, M., Lukina, E., Gusev, D., Mason, P., Wagstaff, P., 2013. Impact of material structure on the fatigue behaviour of NiTi leading to a modified Coffin-Manson equation, *Mater. Sci. Eng. A*. 585, 356–362.
- Lagoudas, D.C., Miller, D.A., Rong, L., Kumar, P.K., Thermomechanical fatigue of shape memory alloys, *Smart Mater. Struct.* 18 (2009) 085021
- Maletta, C., Sgambitterra, E., Furgiuele, F., Casati, R., Tuissi, A., 2012. Fatigue of pseudoelastic NiTi within the stress-induced transformation regime : a modified Coffin – Manson approach, *Smart Mater. Struct.* 112001.
- Meggiolaro, M., 2004. Statistical evaluation of strain-life fatigue crack initiation predictions, *Int. J. Fatigue* 26, 463–476.
- Melton, K., Mercier, O., 1979. Fatigue of NiTi thermoelastic martensites, *Acta Metall.* 27, 137–144.
- Miyazaki, S., Otsuka, K., Suzuki, Y., 1981a. Transformation pseudoelasticity and deformation behavior in a Ti-50.6 at% Ni alloy, *Scripta Metall.* 15, 287–292
- Miyazaki, S., Imai, T., Suzuki, Y., 1981b. Luders-like Deformation Observed in the Transformation Pseudoelasticity of a Ti-Ni Alloy, *Scripta Metall.* 15, 853–856.
- Miyazaki, S., Mizukoshi, K., Ueki, T., Sakuma, T., Liu, Y., 1999. Fatigue life of Ti – 50 at .% Ni and Ti – 40Ni – 10Cu ( at .%) shape memory alloy wires, *Mater. Sci. Eng. A*. 273-275, 658–663.
- Olbricht, J., Yawny, A., Condó, A.M., Lovey, F.C., Eggeler, G., 2008. The influence of temperature on the evolution of functional properties during pseudoelastic cycling of ultra fine grained NiTi. *Mater.Sci. Eng. A* 481-482, 142–145.
- Pelton, A.R., Fino-Decker, J., Vien, L., Bonsignore, C., Saffari, P., Launey M., Mitchell, M.R., 2013. Rotary-bending fatigue characteristics of medical-grade Nitinol wire, *J. Mech. Behav. Biomed. Mater.* 27, 19–32.
- Rahim, M., Frenzel, J., Frotscher, M., Pfetzing-Micklich, J., Steegmüller, R., Wohlschlägel, M., Mughrabi, H., Eggeler, G., 2013. Impurity levels and fatigue lives of pseudoelastic NiTi shape memory alloys, *Acta Mater.* 61, 3667–3686.
- Sawaguchi, T.A., Kausträter, G., Yawny, Y., Wagner, M., Eggeler, G., 2003. Crack initiation and propagation in 50.9 at. pct Ni-Ti pseudoelastic shape-memory wires in bending-rotation fatigue, *Metall. Mater. Trans. A*. 34, 2847–2860.
- Shaw, J. A., Kyriakides, S., 1997. On the nucleation transformation and propagation of phase fronts in a NiTi alloy, 45, 683–700.
- Wagner, M., Sawaguchi, T., Kausträter, G., Höffken, D., Eggeler, G., 2004. Structural fatigue of pseudoelastic NiTi shape memory wires, *Mater. Sci. Eng. A*. 378, 105–109.
- Yawny, A., Sade, M., Eggeler, G., 2005. Pseudoelastic cycling of ultra-fine-grained NiTi shape-memory wires. *Int. J. Mater. Res. (Zeitschrift für Met.)* 96, 608–618.
- Yawny, A., Olbricht, J., Sade, M., Eggeler, G., 2008. Pseudoelastic cycling and ageing effects at ambient temperature in nanocrystalline Ni-rich NiTi wire. *Mater.Sci. Eng. A* 481-482, 86–90.